Physico-chemical properties of macadamia nut shell post-gasification residues and potential agricultural application

Vu Ngoc Linh[1], Nguyen Thu Phuong[2], Le Phuong Thu[3], Dinh Thi Mai Thanh[3], Nguyen Hong Nam[3, *]

[1]*University of Engineering and Technology, Vietnam National University, 144 Xuan Thuy, Cau Giay, Ha Noi, Viet Nam*

[2]*Institute for Tropical Technology, Vietnam Academy of Science and Technology, 18 Hoang Quoc Viet, Cau Giay, Ha Noi, Viet Nam*

[3]*University of Science and Technology of Hanoi, Vietnam Academy of Science and Technology, 18 Hoang Quoc Viet, Cau Giay, Ha Noi, Viet Nam*

[*]Email: *nguyen-hong.nam@usth.edu.vn*

Abstract. In – depth information about the characteristics and potential use of post-gasification residues is the key to unlock the sustainability potential of biomass gasification. This study aimed to explicate the physico-chemical properties of residues after the gasification of macadamia nut shell using a commercial gasifier. The results revealed an important amount of carbon content remained in the residues, marking the low conversion efficiency of the process. The obtained residues were deemed unsuitable for use as adsorbents due to low surface areas with non-porous structures. However, the surface of the residues contained multiple carboxyl and hydroxyl functional groups. Also, a remarkable amount of K (up to 86 wt% of the char's total inorganic elements) was observed to be evenly distributed on the char surface. The results solidified the possibility of utilizing the residues as bio-fertilizers, and provided essential data for the development of sustainable energy production processes using macadamia nut shell for gasification.

Keywords: macadamia nut shell, gasification, biochar, physico-chemical characteristics, post-gasification residue.

Classification numbers: 1.3.2, 2.8.3, 3.4.1

1. INTRODUCTION

In many countries, biomass is an abundant resource with great potential and yet currently neglected. Advanced renewable energy technologies, like gasification, provide a suitable use of biomass as feedstock [1]. With syngas, which mainly consists of CO and H_2, being its primary product, biomass gasification is a vastly beneficial thermal chemical conversion process. Such a claim is supported by the wide variety of applications that syngas has to offer as an excellent energy carrier and chemical precursor [2]. Therefore, in recent years, gasification technology has attracted the attention of many investors and countries around the world [3]. The gasification

process is divided into four consecutive phases: dehydration, pyrolysis, volatile matters decomposition, and char gasification. Primarily, the biomass is heated and then pyrolyzed. Subsequently, the generated substances and the gasifying agents interact to produce the final output of the process.

Nevertheless, the sustainable development of gasification technology depends on two major factors: (1) the diversification of raw materials and (2) the use of solid waste generated from the gasification process [4]. The current state-of-the-art biomass gasification systems are strictly fitted for the consumption of wood and woody materials [2, 5]. The diversification of gasification feedstocks is crucial to the future of this technology due to the intensifying contest for wood [2]. Besides, biomass gasification often generates a large amount of solid waste due to the characteristics of biomass (low conversion efficiency, high ash content) [4]. Therefore, if not properly treated, this end-of-pipe waste can have a great impact on the environment, reducing the reliability of the gasification technology. To identify the most effective and relevant applications, it is necessary to conduct a comprehensive study on the characteristics of the post-gasification residues.

Macadamia nuts are a high value agricultural product that is cultivated globally. The Macadamia tree was first introduced to Viet Namin 1994, and commercially cultivated from 2004 in the North-Western and Central Highlands region of Vietnam. Nevertheless, Viet Nam is also aiming to enlarge its macadamia production in the upcoming years [6]. Thus, macadamia processing activity in Viet Namgenerates a considerable amount of macadamia nut shell (MNS) annually. Unfortunately, due to the lack of suitable application, most of the MNS becomes waste, negatively impacting the environment. Considering the wood-like characteristics of MNS, this biomass would be a potential feedstock for gasification [7].

Therefore, in this study, we demonstrated the first comprehensive study of the physico-chemical, and structural properties of the post-gasification residues of MNS generated via a commercial gasifier and identified its potential applications.

2. MATERIALS AND METHODS

2.1. Macadamia husk feedstock

For this study, MNS from the 695 (Beaumont) macadamia variety (Figure 1) was selected as it is one of the most widely cultivated varieties in Viet Nam. MNS was obtained from Dak Lak province in the Central Highlands region of Viet Nam.
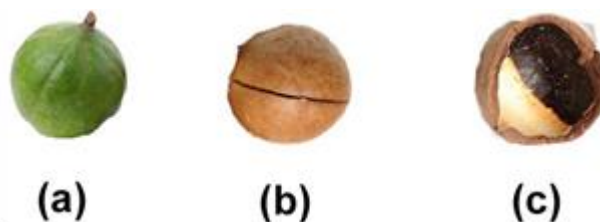

Figure 1. (a) Macadamia fruit, (b) Fresh MNS, (c) Dried MNS

After being rinsed with distilled water and subsequently sun-dried, the MNS samples were maintained at room temperature in air-tight boxes before going through further treatment and analysis.

2.2. Collection of post-gasification residues

The solid residues were collected after gasification of MNS using a commercial gasifier (PP20 All Power lab) (Figure 2). The system comprises of a gasifying unit, a filtration module, and a gas combustion engine. An auger, where the dehydration and pyrolysis stage occur, is installed at the top of the reactor to introduce the feedstock into the gasifier. Air, pre-heated by the generated syngas, is fed into the reactor through nozzles to create a combustion zone where the pyrolysis tars are oxidized. Consequently, the outlet gases from the combustion zone react with the char from the reduction zone, which result in the production of the fuel gases. Eventually, the residual char is discarded via another auger. A cyclone is implemented to separate the reactor's outgoing syngas and fine particles. Subsequently, the syngas runs through a built-in char bed filter to rid itself of tars, moisture, and particulates. Ultimately, the filtered syngas is combusted in the engine, which is incorporated with an alternator for power generation. In this study, the generator was connected to several spatial heaters that were used as electrical load, syngas is combusted in the engine, which is incorporated with an alternator for power generation. In this study, the generator was connected to several spatial heaters that were used as electrical load.

Primarily, the hopper was loaded with roughly 100 kg of raw feedstock. For the activation of the gasifier, a propane gas torch was used to heat the reduction zone to 80 $^{\circ}$C. Throughout this phase, the outlet syngas was channeled to the flare. The engine automatically started once the temperature exceeded 700 $^{\circ}$C, after about 20 minutes. The electrical load was increased progressively until reaching the appropriate level. After approximately 2 hours of operation, the system obtained steady-state. The system was halted and left to cool down naturally upon the depletion of the feedstock. Ultimately, as the system was shutting down, the electrical load was progressively brought down until the engine ceased with the syngas being directed to the flare. Marking the end of the experiment, the air inlet was closed. The residues were retrieved from two sections: the lower site of the reactor (Residue 1), and the end-of-pipe biochar container (Residue 2).

Figure 2. The commercial PP20 gasifier

2.3. Proximate analysis

In this study, proximate analysis of MNS post-gasification residues was thoroughly conducted and reported. The ash (A) (ASTM D-3174 standard), and volatile matter (V) (ASTM D-3175 standard) were investigated. Apart from that, the higher heating value (HHV) of MNS was identified using a Parr 6200 Calorimeter. Consequently, the fixed carbon content (FC) was quantified by $FC = 100 - VM - A$.

2.4. Char surface functional groups analysis

With the MIR range of 500-4000 cm^{-1} and the resolution of 4 cm^{-1}, a UATR-FTIR spectrometer (PerkinElmer-) facilitated the identification of the functional groups on the surface of MNS post-gasification residues. The atmospheric humidity was regulated below 50 % via an independent dehumidifier. The samples were uniformly ground before the analysis. Each sample was scanned twice under a compression force of 40 N.

2.5. Char elemental compositional analysis

A JSX-1000S X-ray fluorescence spectrometer (XRF) developed by Jeol was utilized for the elemental composition analysis of the post-gasification residues. The apparatus was equipped with silicon drift detector, and an optical system with filters that facilitated highly sensitive analysis of the entire energy range. Lighter elements in the samples were identified in a vacuum chamber.

2.6. Surface chemical compositions and distribution

A scanning electron microscopy (TM4000Plus Hitachi) incorporated with an energy-dispersive X-ray spectroscopy (EDS) analysis allowed the investigation of the surface chemical compositions and distribution of the post-gasification residues. An assessment of the surface chemical distribution was enabled via the mapping of the surface chemical compositions.

2.7. N_2 adsorption/desorption analysis

The BET–NOVA touch LX4 of Quantachrome was used to determine the N_2 adsorption/desorption of the MNS post-gasification residues. Prior to the analysis, the samples were outgassed for 6 hours at 300 $^{\circ}C$. Throughout the process, the yielded data were tracked and logged throughout a range of p/p_o from 0 to 0.99. Consequently, an estimation of the residues' total surface area and total pore volume was obtained using the Brunauer – Emmett – Teller (BET) method, and the density functional theory (DFT) method.

3. RESULTS AND DISCUSSION

3.1. Proximate characteristics of post-gasification residues

Important proximate characteristics of the post-gasification residues, namely fixed carbon, ash content, volatile matter, and calorific value were investigated. The results of the analysis were presented in Table 1. The volatile matter remained in both residues was very low (2 - 3 %), as a result of the conversion under high temperatures. On the contrary, the ash content and fixed-carbon content changed dramatically when being submitted to the thermal decomposition during gasification. Residue 1 possesses an ash content of 20.2 %, which is much lower than that of

Residue 2 (45.5 %). The high ash content is a major obstacle in finding suitable applications for Residue 2. The HHV of Residue 1 was 28.2 MJ kg^{-1}, which is similar with that of typical coal [8]. The HHV values of residues could be considered as an essential input in the computation of heat balance, modeling, and simulations; thus, contribute in the determination of the capacity and dimensions of the energy conversion systems. It is noteworthy that both residues still contain a large amount of carbon content, marking the incomplete conversion of the gasification process. This fact is not an advantage in terms of energy conversion, but could be beneficial for the use of the residue as a biochar product.

Table 1. Proximate characteristics of post-gasification residues.

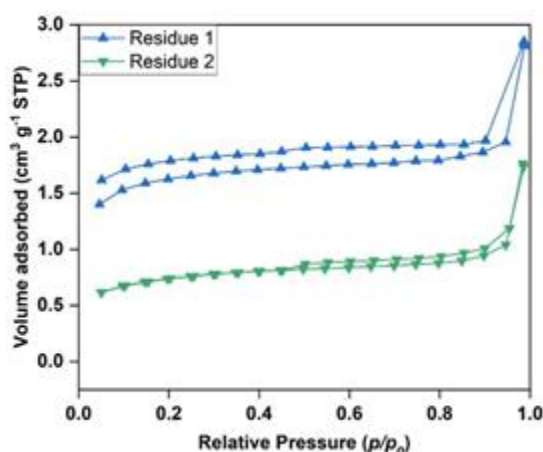| Parameter	VM_{db} (wt%)	A_{db} (wt%)	FC_{db} (wt%)	HHV (MJ kg^{-1})
Residue 1	3.1	20.2	76.7	28.2
Residue 2	2.1	45.5	52.4	15.1

3.2. Porosity of post-gasification residues

Figure 3. N_2 adsorption/desorption of post-gasification residues.

Table 2. Specific surface area and total pore volume of residues from gasification.

Sample	S_{BET} (m^2 g^{-1})	V_{Total} (cm^3 g^{-1})
Residue 1	5.42	0.045
Residue 2	3.38	0.029

The N_2 adsorption/desorption isotherms of MNS post-gasification residues were displayed in Figure 3. The result showed that the residues adsorbed an insignificant amount of N_2. Table 2 showed the estimation of the S_{BET} and V_{Total} achieved by the BET and DFT methods. The S_{BET} and V_{Total} of Residue 1 reached $S_{BET} = 5.42$ m^2 g^{-1} and $V_{Total} = 0.045$ cm^3 g^{-1}, and Residue 2 reached $S_{BET} = 3.38$ m^2 g^{-1} and $V_{Total} = 0.045$ cm^3 g^{-1}. These results implied that both the residues

possess a non-porous structure. Thus, the MNS post-gasification residues could be deemed unfit for application as adsorbents.

3.3. Surface functional groups of post-gasification residues

Figure 4 illustrated different functional groups on the surface of the residues. The compositions of functional groups on the post-gasification residues surface bring about essential insight on the char properties, and reaction mechanisms [9]. The FTIR spectra indicated that the surface of both residues contains similar functional groups on the surface, but their intensity was much stronger in Residue 1 than Residue 2. The first peak (around 1000 cm^{-1}) corresponded to the C-O groups while the second peak (around 1308 cm^{-1}) attributed to the O-H groups. The third peak at 1640 cm^{-1} implied the presence of the C=C stretching bonds. Nevertheless, the fourth and fifth peaks at 2263 and 3000 cm^{-1} suggested the existence of C=O and C-H groups on the surface of the residues, respectively. A small trace of O–H group was also observed in both residues.
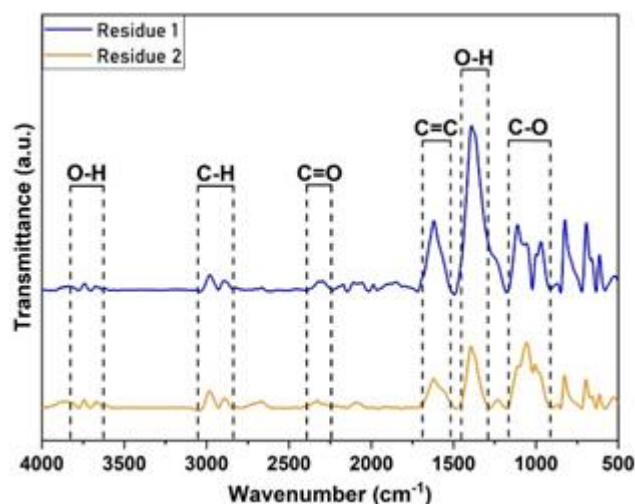

Figure 4. FTIR spectra of post-gasification residues

In general, the surface of MNS post-gasification residues contains mostly carboxyl and hydroxyl functional groups, which tend to form salts with metallic cations in solid residue [10, 11]. As the result, these salts improve the alkalinity of the solid residues along with the cation exchange capacity in soil. Thus, MNS post-gasification residues could be considered beneficial if used as a soil amendment [12].

3.4. Evolution in elemental compositions

Via the XRF technique, the elemental compositions of the post-gasification residues were investigated. The XRF spectra of MNS post-gasification residues was displayed in Figure 5. It can be observed that a large amount of K, ranging from 80 to 86 wt.% (of the total inorganic elements) exists in both residues. The determined K content of the MNS post-gasification residues is substantially higher than that of other common biomasses in Viet Nam[13–16]. For example, biochar derived from tea waste (2.93 wt.%), hazelnut husk (1.38 wt.%), rice husk (2.13 wt.%), and poultry litter (8.66 wt.%) were found to possess significantly lower amount of K

content compare to that of MNS char [14]. Moreover, the amount of K detected in elephant grass, which was dominant among its inorganic content, was considerably inferior to that of MNS post-gasification residues [13]. Such result may give interesting hints about the possible applications of MNS post-gasification residues.
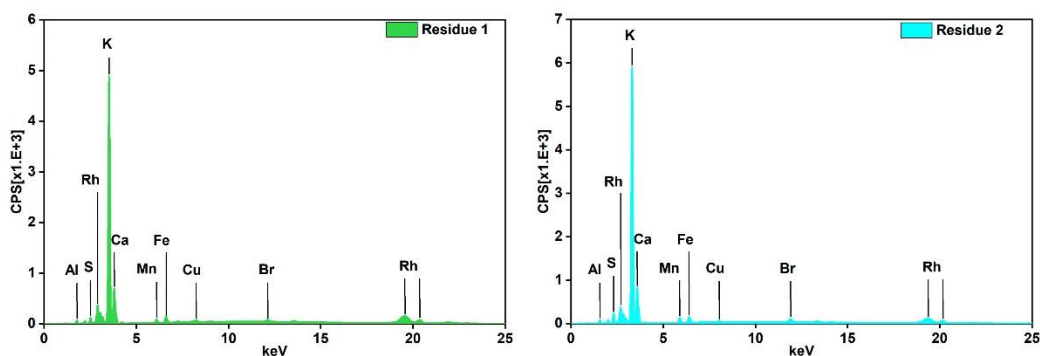

Figure 5. XRF spectra of post-gasification residues.

Previous studies have highlighted the importance of K to plant growth, crop production, soil microorganisms, human's and livestock's well-being [17]. With such remarkable K-content, the MNS post-gasification residues could be considered as low-cost, and sustainable bio-fertilizers. This is especially beneficial as the increasing scarcity of mineral ores makes K fertilizers become more and more costly [18]. Furthermore, different metals, namely aluminum, chromium, iron, copper, and rhodium, as well as non-metal elements, namely phosphorus, calcium, and bromine, were also identified. Such minerals are also serviceable to plant growth. Apart from that, no heavy metal was found in the post-gasification residue samples. This might be a foundation for the production of a sustainable MNS biochar.

3.5. Mapping of surface elements on post-gasification residues
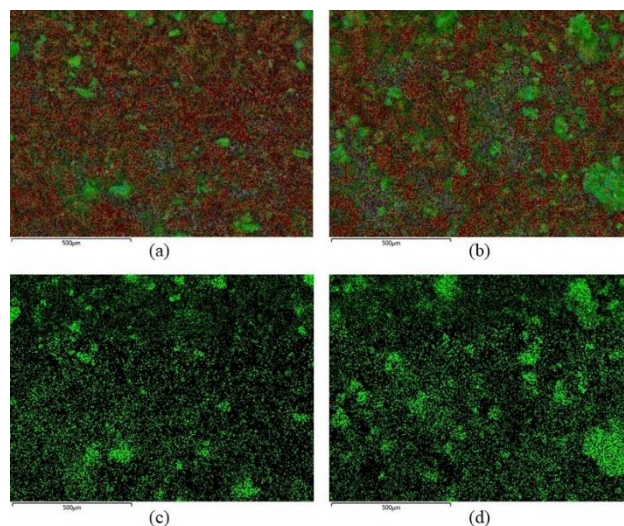

Figure 6. Mapping images of all surface elements in (a) Residue 1 and (b) Residue 2; Mapping of K element only in (c) Residue 1 and (d) Residue 2. In red: C element; In green: K element.

Figure 6a and Figure 6b presented the mapping images of all surface elements in post-gasification residues. It can be seen that C (in red color) and K (in green color) were the two dominant elements on the surface of the residue. Considering the K content alone in Residue 1 (Figure 6c) and Residue 2 (Figure 6d), it can be seen that the K element was evenly distributed on the surface of both Residues. This is greatly beneficial to the absorption of K by plants if these chars were used as soil amendments. Previous studies have pointed out that the absorption of K from biochar does not solely depend on the proportion of this element in the char but also the accessibility to K of the plant. In many cases, despite the high K content, plants were unable to absorb the nutrient as K was entrapped within the rigid phytolith, which is commonly found in biochar [19]. Regarding MNS post-gasification residues, the significant presence of K on the surface might result in an easier and more efficient release of the nutrient, thus better improve soil quality.

4. CONCLUSIONS

An extensive database of the physico-chemical and structural properties of MNS post-gasification residues was established in this study. The high amount of fixed carbon on the residues marked the incomplete conversion of the biomass, leaving behind a rich-organic carbonaceous material after gasification. Considering an insignificant porosity and a high ash content, the use of post-gasification residues as absorbents seems to be irrelevant. However, the presence of carboxyl and hydroxyl functional groups caused by the gasifying reactions between MNS char and the reacting agents, combined with the remarkably large amount of K (up to 86 wt% of the total inorganic elements) evenly distributed on the surface of the solid residue suggested that it has promising potential to be utilized as fertilizer and soil amendment.

CRediT authorship contribution statement: Vu Ngoc Linh: Data curation, investigation, writing – original draft, Nguyen Thu Phuong: Formal analysis, investigation, Le Phuong Thu: Formal analysis, investigation, Dinh Thi Mai Thanh: Funding acquisition, resources, validation, Nguyen Hong Nam: Conceptualization, methodology, supervision, writing – review and editing.

Declaration of competing interest. The authors declare that they have no known competing financial interests or personal relationships that could have appeared to influence the work reported in this paper.

REFERENCES

1. Dahou T., Defoort F., Nguyen H. N., Bennici S., Jeguirim M., Dupont C. - Biomass steam gasification kinetics: relative impact of char physical properties vs. inorganic composition, Biomass Conv. Bioref. **12** (2022) 3475-3490. https://doi.org/10.1007/s13399-020-00894-9

2. Nguyen H. N., Van De Steene L. - Steam gasification of rice husk: effects of feedstock heterogeneity and heat-mass transfer, Energ. Source. Part A **0** (2019) 1-15. https://doi.org/10.1080/15567036.2019.1694104

3. Nguyen H. N., Steene L. V. D., Le T. T. H., Le D. D., Ha-Duong M. - Rice Husk Gasification: from Industry to Laboratory, IOP C. Ser. Earth Env. **159** (2018) 012033. https://doi.org/10.1088/1755-1315/159/1/012033

4. Nguyen H. N., Nguyen P. L. T., Tran V. B. - Zero-waste biomass gasification: Use of residues after gasification of bagasse pellets as CO2 adsorbents, Therm. Sci. Eng. Prog. **26** (2021) 101080. https://doi.org/10.1016/j.tsep.2021.101080

5. Hong Nam N. - Complete Parametric Study of Bagasse Pellets During High-Temperature Steam Gasification, J. Therm. Sci. Eng. Appl. **12** (2019). https://doi.org/10.1115/1.4045698

6. Reuters. Vietnam to rapidly expand macadamia farms as demand rises. https://www.reuters.com/article/vietnam-macadamia-idUKL3N2GL2K5

7. Conesa J. A., Sakurai M., Antal M. J. - Synthesis of a high-yield activated carbon by oxygen gasification of macadamia nut shell charcoal in hot, liquid water, Carbon **38** (2000) 839-848. https://doi.org/10.1016/S0008-6223(99)00182-7

8. Tan P., Zhang C., Xia J., Fang Q. Y., Chen G. - Estimation of higher heating value of coal based on proximate analysis using support vector regression, Fuel Process. Technol. **138** (2015) 298-304. https://doi.org/10.1016/j.fuproc.2015.06.013

9. Mai N. T., Nguyen M. N., Tsubota T., Nguyen P. L. T., Nguyen N. H. - Evolution of physico-chemical properties of Dicranopteris linearis-derived activated carbon under various physical activation atmospheres, Sci. Rep. **11** (2021) 14430. https://doi.org/10.1038/s41598-021-93934-x

10. Xu R., Zhao A., Yuan J., Jiang J. - pH buffering capacity of acid soils from tropical and subtropical regions of China as influenced by incorporation of crop straw biochars, J. Soils Sediments **12** (2012) 494-502. https://doi.org/10.1007/s11368-012-0483-3

11. Yuan J. H., Xu R. K., Zhang H. - The forms of alkalis in the biochar produced from crop residues at different temperatures, Bioresource Technol. **102** (2011) 3488-3497. https://doi.org/10.1016/j.biortech.2010.11.018

12. Hussain R., Garg A., Ravi K. - Soil-biochar-plant interaction: differences from the perspective of engineered and agricultural soils B, Eng. Geol. Environ. **79** (2020) 4461-4481. https://doi.org/10.1007/s10064-020-01846-3

13. Adeniyi A. G., Ighalo J. O., Onifade D. V. - Production of biochar from elephant grass (Pernisetum purpureum) using an updraft biomass gasifier with retort heating, Biofuels, **12** (2021) 1283-1290. https://doi.org/10.1080/17597269.2019.1613751

14. Akça M. O., Ok S. S., Deniz K., Mohammedelnour A., Kibar M. - Spectroscopic Characterisation and Elemental Composition of Biochars Obtained from Different Agricultural Wastes, J. Agr. Sci. **27** (2021) 426-435. https://doi.org/10.15832/ankutbd.623876

15. Hossain N., Nizamuddin S., Griffin G., Selvakannan P., Mubarak N. M., Mahlia T. M. I. - Synthesis and characterization of rice husk biochar via hydrothermal carbonization for wastewater treatment and biofuel production, Sci. Rep. **10** (2020) 18851. https://doi.org/10.1038/s41598-020-75936-3

16. Khawkomol S., Neamchan R., Thongsamer T., Vinitnantharat S., Panpradit B., Sohsalam P., Werner D., Mrozik W. - Potential of Biochar Derived from Agricultural Residues for

Sustainable Management, Sustainability **13** (2021) 8147. https://doi.org/10.3390/su13158147

17. Ghulam Mustafa Kubar K. H. T., Shahneela Khashkhali M. M. N., Kubar M. S., Kubar K. A., Kubar A. A. - 27. Effect of potassium (K+) on growth, yield components and macronutrient accumulation in Wheat crop, Pure Appl. Biol. **8** (2019) 248-255.

18. Kumar S., Diksha Sindhu S. S., Kumar R. - Biofertilizers: An ecofriendly technology for nutrient recycling and environmental sustainability, Curr. Res. Microbial Sci. **3** (2022) 100094. https://doi.org/10.1016/j.crmicr.2021.100094

19. Tran C. T., Mai N. T., Nguyen V. T., Nguyen H. X., Meharg A., Carey M., Dultz S., Marone F., Cichy S. B., Nguyen M. N. - Phytolith-associated potassium in fern: characterization, dissolution properties and implications for slash-and-burn agriculture, Soil Use Manage. **34** (2018) 28-36. https://doi.org/10.1111/sum.12409